

## Physics Issues for a Very-Low-Aspect-Ratio Quasi-Poloidal Stellarator (QPS)

J. F. Lyon 1), L. A. Berry 1), S. P. Hirshman 1), D. A. Spong 1), D. J. Strickler 1),  
 P. K. Mioduszewski 1), B. E. Nelson 1), D. E. Williamson 1), A. S. Ware 2), E. Barcikowski 2),  
 A. J. Deisher 2), A. Brooks 3), G. Y. Fu 3), D. Mikkelsen 3), D. A. Monticello 3),  
 N. Pomphrey 3), R. Sanchez 4)

1) Oak Ridge National Laboratory, P.O. Box 2009, Oak Ridge, TN 37831-8072, U.S.A.

2) University of Montana-Missoula, Missoula, Montana 59812, U.S.A.

3) Princeton Plasma Physics Laboratory, P.O. Box 451, Princeton, NJ 08502, U.S.A.

4) Universidad Carlos III de Madrid, Madrid, Spain

e-mail contact of main author: lyonjf@ornl.gov

**Abstract.** A quasi-poloidal stellarator with very low plasma aspect ratio ( $R/a \sim 2.7$ ,  $1/2$ - $1/4$  that of existing stellarators) is a new confinement approach that could ultimately lead to a high-beta compact stellarator reactor. The Quasi-Poloidal Stellarator (QPS) experiment is being developed to test key features of this approach. The QPS will study neoclassical and anomalous transport, stability limits at beta up to 2.5%, the configuration dependence of the bootstrap current, and equilibrium robustness. The quasi-poloidal symmetry leads to neoclassical transport that is much smaller than the anomalous transport. The reduced effective field ripple may also produce reduced poloidal viscosity, enhancing the ambipolar  $E \times B$  poloidal drift and allowing larger poloidal flows for reduction of anomalous transport. A region of second stability exists in the QPS experiment at higher beta. Very-high-beta configurations with a tokamak-like transform profile have also been obtained with a bootstrap current  $1/3$ - $1/5$  that in an equivalent tokamak. These configurations are stable to low- $n$  ideal MHD kink and vertical instabilities for beta up to 11%. Ballooning-stable configurations are found for beta in the range 2% to 23%.

### 1. Introduction

For exact poloidal ( $\theta$ ) symmetry, the canonical angular momentum  $p_\theta$  is conserved and: (1) the orbit excursions from a flux surface are limited to the gyroradius in the *toroidal* magnetic field  $\rho_T$  rather than in the *poloidal* magnetic field  $\rho_p$  (the banana width) where  $\rho_T \ll \rho_p$ ; (2) there is no flow damping in the poloidal direction; and (3) the bootstrap current is reduced by  $1/N$  where  $\iota$  is the rotational transform ( $= 1/q$ ) and  $N$  is the number of field periods. While exact poloidal symmetry is not possible in a three-dimensional magnetic configuration, approximate quasi-poloidal symmetry (qps) in which the dominant components in the magnetic field  $|B|$  spectrum are poloidally symmetric in flux coordinates results in small  $\mathbf{B} \times \nabla B$  drifts out of a flux surface and reduced neoclassical transport relative to nonsymmetric stellarators, reduced flow damping in the poloidal direction, and reduced neoclassical bootstrap current relative to axisymmetric configurations. The reduced bootstrap current can lead to high- $\beta$  MHD stability limits. Two types of low-aspect-ratio qps configurations are discussed: (1) the Quasi-Poloidal Stellarator (QPS) experiment with a stellarator rotational transform profile and small plasma current [1], and (2) very-high- $\beta$  hybrid configurations with moderate plasma current and a tokamak-like rotational transform profile [2].

### 2. The Quasi-Poloidal Stellarator Experiment

The QPS experiment currently under design is a quasi-poloidal stellarator that is designed to test key features of this approach. QPS has very low plasma aspect ratio  $A = \langle R \rangle / \langle a \rangle \approx 2.7$ ,  $1/2$ - $1/4$  that of existing stellarators, where  $\langle R \rangle$  and  $\langle a \rangle$  are the average major and minor radii of the non-

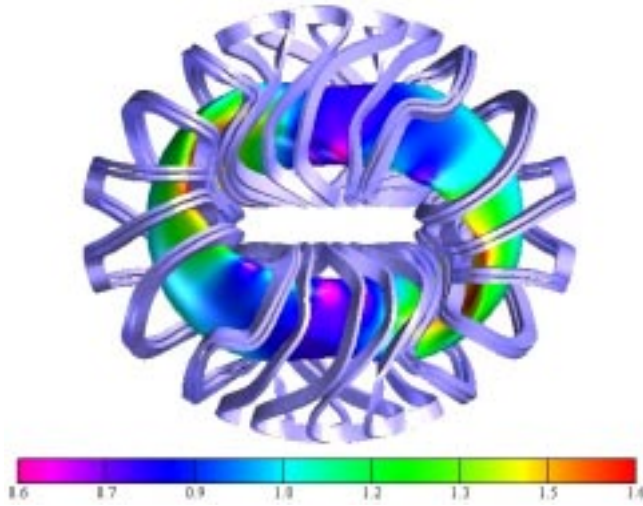


FIG. 1. Top (left) and side (above) views of the QPS plasma and the modular coils that create it. The colors indicate contours of  $|B|$  in T on the last closed flux surface.

circular and non-axisymmetric plasma. The shape of the QPS flux surfaces shown in Fig. 1 varies from bean-shaped at the higher-field ends to D-shaped in the middle of the long straight sections. A non-planar (helical) variation of the magnetic axis is also indicated in Fig. 1. The open coil geometry allows good access between the coils for plasma heating and diagnostics.

A cutaway view of QPS is shown in Fig. 2 and the main device parameters are listed in Table 1. The main coil set has two field periods with 8 modular coils per period. Due to stellarator symmetry, only four different coil types are needed. The two winding packs that form the coils are separated by a thin stainless steel structural "T" except in the center of the long section where the windings follow independent paths (with a wider "T") to improve the configuration properties. The modular coils have a stainless steel vacuum-tight case since they share the same vacuum as the plasma. The central bore contains the central legs of the twelve TF coils. The two sets of vertical field coils and a central solenoid allow plasma shape and position control and driving up to 150 kA of plasma current. Twelve 61-cm-diameter ports around the midplane and smaller ports

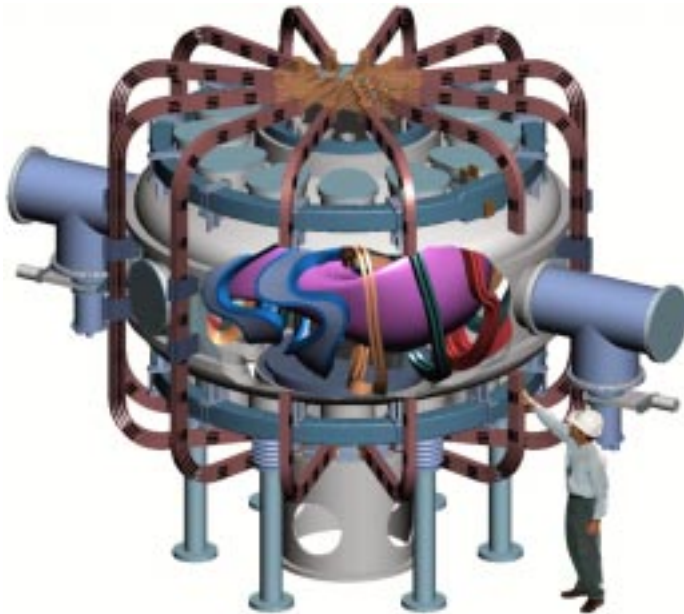


Fig. 2. Cutaway view of QPS.

TABLE I. QPS PARAMETERS

Ave. major radius $\langle R \rangle$	0.9 m
Ave. plasma radius $\langle a \rangle$	0.33 m
Plasma aspect ratio	2.7
Plasma volume $V_{\text{plasma}}$	2 m <sup>3</sup>
Central, edge rotational transform $\iota_0, \iota_a$	0.21, 0.32
Average field on axis from modular coils	$B_{\text{mod}} = 1$ T for 1-s pulse
Auxiliary toroidal field	$\pm 0.2$ T
Ohmic current $I_{\text{plasma}}$	$\leq 150$ kA
ECH power	0.6-1.2 MW
ICRF heating power	1-3 MW

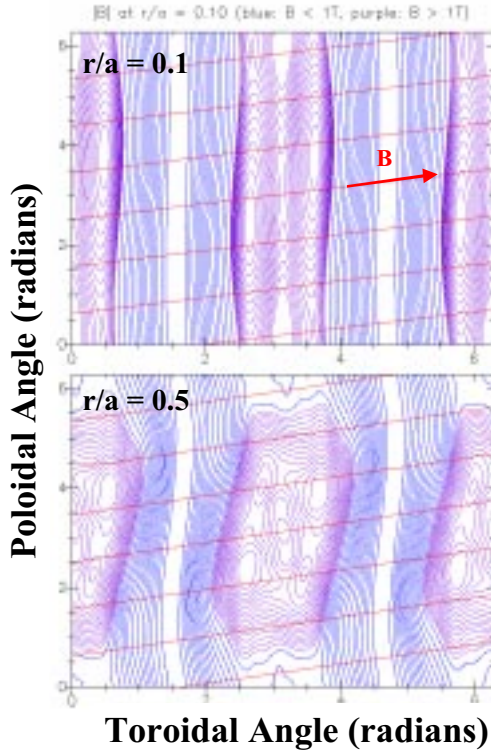


Fig. 3.  $|B|$  contours and field lines in QPS.

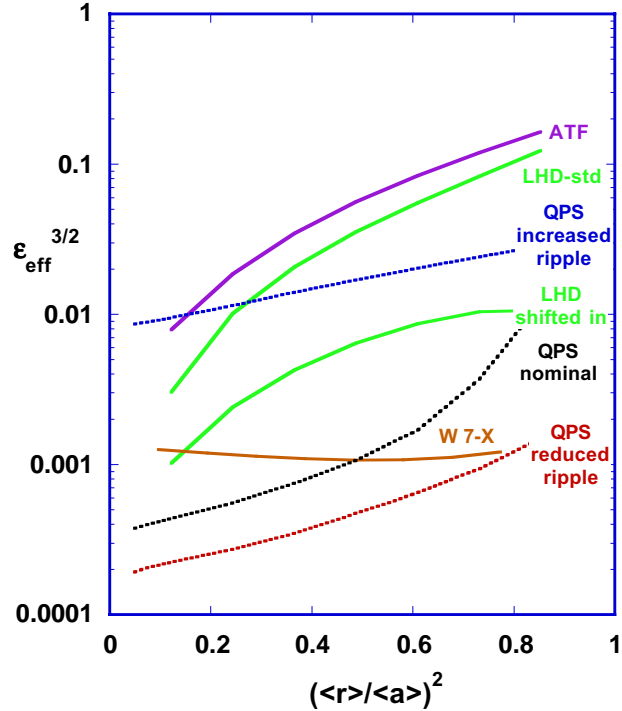
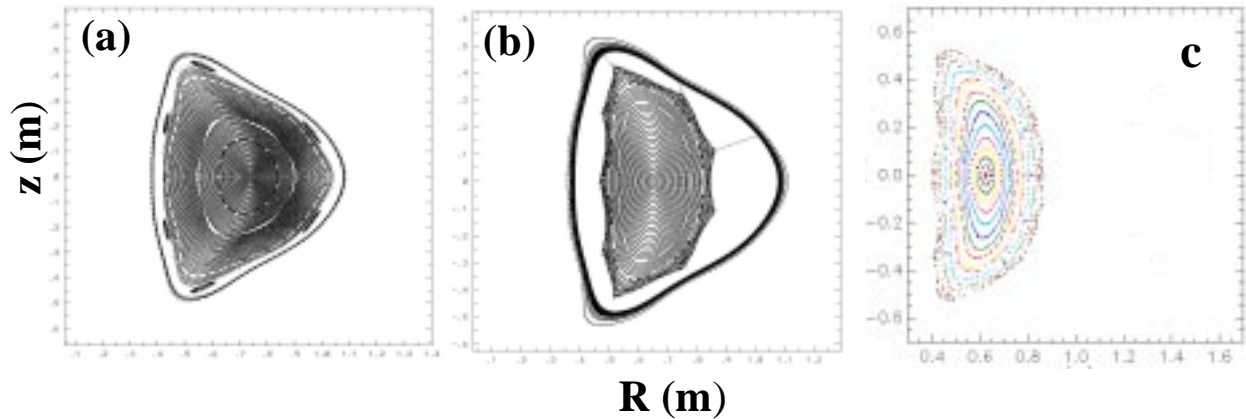


Fig. 4. Coefficient of thermal diffusivity in the  $1/\nu$  regime for different stellarators and the variation possible in QPS.

on the top and bottom of the vacuum tank provide access for heating, diagnostics, coil services, and instrumentation. Field lines leave the plasma predominantly at the top and bottom of the bean-shaped cross sections where recycling neutrals would be confined by divertor baffles and reionized in the boundary plasma. Connection lengths are long enough for an effective divertor.

Figure 3 shows contours of  $|B|$  on two flux surfaces in flux coordinates in which the magnetic field lines (shown in red) are straight. The degree of quasi-poloidal symmetry varies with plasma radius. In the plasma core ( $r/\langle a \rangle < 1/2$ ) the magnetic energy in non-poloidally symmetric field components is  $<10\%$  of that in the poloidally symmetric field components and rises to  $\sim 30\%$  at the plasma edge.  $\mathbf{B}$  and  $\nabla B$  are more closely aligned than is possible with other forms of symmetry; this reduces banana widths and radial particle drifts out of a flux surface over most of the plasma cross section. Near the edge close alignment of globally averaged drift surfaces and flux surfaces (quasi-omnigenity) occurs that helps to reduce neoclassical transport.

A measure of the reduction in neoclassical transport is shown in Fig. 4. For  $E_r = 0$  in the low-collisionality limit, the neoclassical ripple-induced heat diffusivity is proportional to  $\epsilon_{\text{eff}}^{3/2}$  where  $\epsilon_{\text{eff}}$  is the effective ripple in a single-helicity  $1/\nu$  transport model that gives the same transport as a full 3-D calculation in this limit. QPS has similar transport to that in the W 7-X configuration, but at  $1/4$  the plasma aspect ratio. Reducing  $\epsilon_{\text{eff}}^{3/2}$  further in QPS would not be effective since the implied energy confinement time due to purely neoclassical losses would greatly exceed the ISS-95 stellarator confinement scaling, and other losses would likely be dominant. The high degree of quasi-poloidal symmetry and the reduced effective field ripple may also produce reduced poloidal viscosity, enhancing the naturally occurring  $\mathbf{E} \times \mathbf{B}$  poloidal drifts and allowing larger poloidal flows for possible shear damping reduction of anomalous transport.



**Fig. 5.** Magnetic surfaces at the D symmetry plane for  $\langle\beta\rangle = 2\%$  (a) and  $\beta = 0$  (b) for the same coil currents and (c) for different coil currents. The outer curve is 5% larger than the VMEC 2%  $\beta$  boundary.

While the QPS experiment is designed to study regimes in which either anomalous transport or neoclassical transport is dominant, it can also test stability limits at  $\langle\beta\rangle \sim 2.5\%$ , the configuration dependence of the bootstrap current, and equilibrium robustness at finite beta. The QPS magnetic configuration is relatively robust for increasing  $\beta$ , as shown in Fig. 5; only small magnetic islands are seen that should be healed by the bootstrap current. The plasma is Mercier stable for  $\langle\beta\rangle \sim 2.5\%$ . The MHD stability limit for QPS is theoretically set by infinite- $n$  ballooning modes at  $\beta \sim 2\%$ , although experiment and recent finite- $n$  ballooning calculations indicates that this should not be a limit. Trapped particles are localized in the long low curvature regions, which should improve stability to dissipative trapped electron modes. Kink and vertical modes are stable at  $\langle\beta\rangle \sim 5\%$  without feedback or close conducting walls. The stellarator rotational transform and bootstrap current should suppress magnetic islands and neoclassical tearing modes.

Infinite- $n$  ballooning modes are unstable for  $\langle\beta\rangle = 2.5\text{--}5.5\%$  in QPS, but stable at higher  $\beta$ . Figure 6 shows a QPS configuration with  $\beta = 9.6\%$ . The colors indicate contours of constant  $|B|$ . As  $\beta$  is increased above 2%, the plasma becomes ballooning unstable. At higher  $\beta$  ( $\beta > 6\%$ ), the core plasma enters a region of second stability. This region of second stability grows as  $\beta$  is increased until at the highest  $\beta$  ( $\beta = 9.6\%$ ) only a few surfaces near the edge remain unstable.

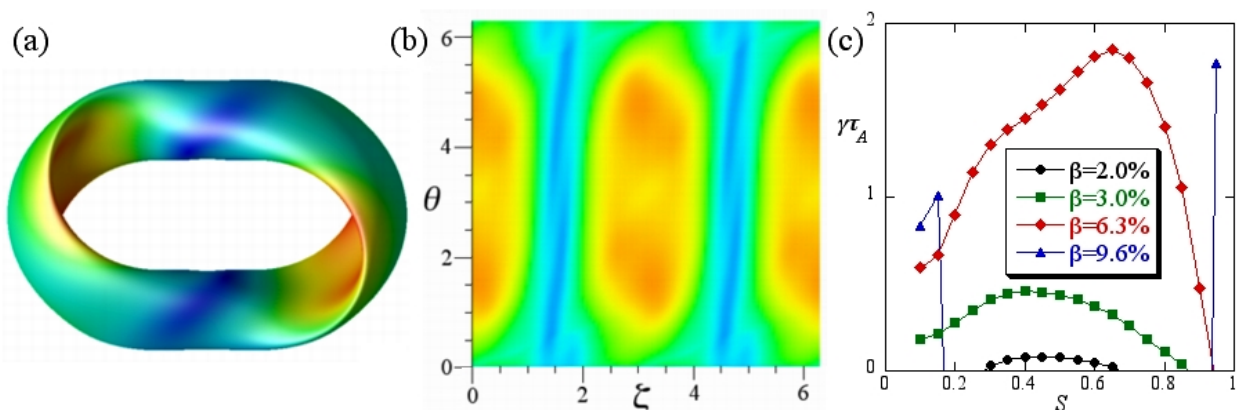


**Fig. 6.** (a) The last closed flux surface of a QPS experiment reference case with (b) contours of  $|B|$  in flux coordinates for the  $(r/a)^2 = 0.75$  surface and (c) normalized ballooning growth rates for a range of  $\beta$ .

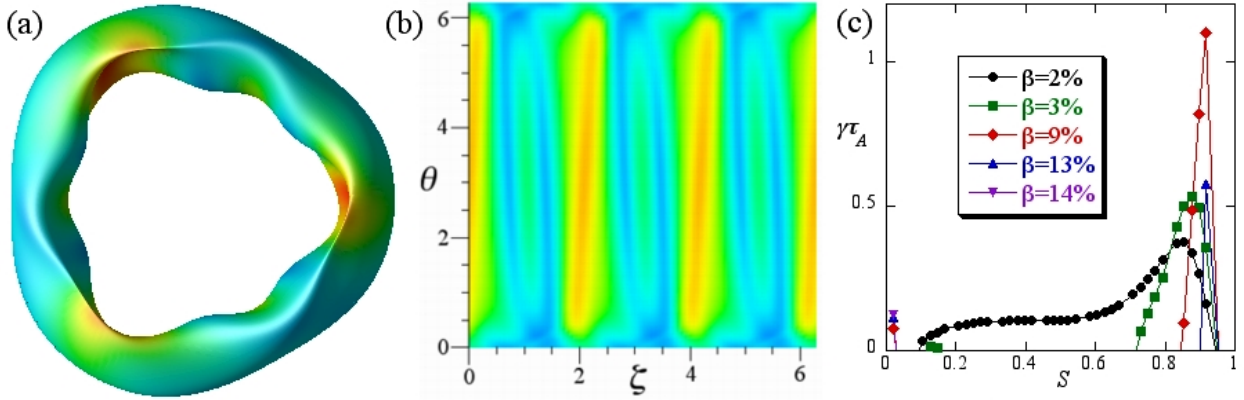


Fig. 7. (a) The last closed flux surface of a three-field period,  $\beta = 15\%$ ,  $A = 3.7$ , qps configuration with (b) contours of  $|B|$  in flux coordinates for the  $(r/a)^2 = 0.75$  surface and (c) normalized ballooning growth rates for a range of  $\beta$ .

### 3. High- $\beta$ Quasi-Poloidal Hybrid Configurations

Another type of qps configuration is very-high- $\beta$  hybrid configurations with a high-shear tokamak-like rotational transform profile [ $\iota(0) \sim 0.4$  to  $\iota(a) \sim 0.1$ , primarily from bootstrap current] [2] in contrast to the lower shear stellarator rotational transform profile of the QPS experiment. Unlike usual stellarators, the high- $\beta$  qps stellarator hybrids are distinguished by a relatively small external rotational transform arising from external coils (typically,  $\iota_{\text{coils}} \sim 0.05$ -0.10). The primary symmetry of the high- $\beta$  hybrid cases is similar to the QPS configuration but the dominant symmetry breaking terms are not the same. Figure 7a shows the last closed flux surfaces for a three-field period hybrid qps configuration with  $A = 3.7$  and  $\beta = 15\%$ . Contours of  $|B|$  in flux coordinates are shown in Fig. 7b for the  $(r/a)^2 = 0.75$  surface which display the qps symmetry of this configuration. The degree of quasi-poloidal symmetry increases and the neoclassical transport and fast ion losses decrease as  $\beta$  increases. The non-axisymmetric ( $n \neq 0$ ) Fourier components of  $|B|$  reduce the neoclassical bootstrap current to 1/3-1/5 that in an equivalent tokamak (an axisymmetric configuration with the same  $n = 0$  boundary coefficients), resulting in stability to low- $n$  ideal MHD kink modes for high values of  $\beta$ , up to  $\beta = 11\%$  for kink and vertical stability. At this value of  $\beta$ , the Troyon factor  $\beta_N = \beta(\%) [ \langle a \rangle (m) B(T) / I(\text{MA}) ] = 19$ , which is significantly larger than the  $\beta_N \sim 3$  for kink stability in an equivalent tokamak with no wall stabilization. The infinite- $n$  ballooning and Mercier stability  $\beta$  limit for these qps configurations is very high: Mercier and ballooning-stable configurations with self-consistent bootstrap current were found for plasmas with  $2\% < \beta < 23\%$ . Decreasing beta with fixed shape and rotational transform profile resulted in ballooning-unstable configurations as shown in Fig. 7c for the case with  $\beta = 15\%$ . However, relatively small shape and profile modifications can produce ballooning stable plasmas at all values of  $\beta < 23\%$ .

[1] LYON, J.F., and the QPS team, "QPS, A Low Aspect Ratio Quasi-Poloidal Concept Exploration Experiment", <http://qps.fed.ornl.gov/>, April 2001.

[2] WARE, A.S., et al., "High- $\beta$  Equilibria of Drift Optimized Compact Stellarators", Phys. Rev. Lett. **89** 125003 (2002).

Acknowledgements. Research supported by the U.S. Dept. of Energy under contract DE-AC05-00OR22725 with UT-Battelle, LLC and Grant No. DE-FG03-97ER54423 at Univ. of Montana.